Different effects of 3-week disuse on the phenotype and gene expression of the calf and thigh muscles

Mira A. Orlova[1], Nadia S. Kurochkina[1], Roman Yu. Zhedyaev[1], Nikita E. Vavilov[2], Viktor G. Zgoda[2], Alina A. Puchkova[1], Anna A. Borzykh[1], Tatiana F. Vepkhvadze[1], Egor M. Lednev[1], Pavel A. Makhnovskii[1], Gleb V. Galkin[1], Valery E. Novikov[1], Alexey V. Shpakov[1], Daniil V. Popov[1, *]

1 Institute of Biomedical Problems of the Russian Academy of Sciences, Moscow, Russia

2 V. N. Orekhovich Research Institute of Biomedical Chemistry, Moscow, Russia

* – corresponding author

M.A. Orlova and N.S. Kurochkina have contributed equally to this work.

Abstract

Disuse, like several other pathological conditions, has specific effects on various skeletal muscles; the mechanisms underlying these responses remain unclear. We aimed to compare the disuse-induced changes in the phenotype and proteome of the calf and thigh muscles, and to assess the extent to which these proteomic changes are regulated at the mRNA and other levels. Twelve healthy young males participated in 3-week bed rest. Disuse resulted in a greater decrease in lean mass, aerobic performance, and changes in the proteome and transcriptome of the calf muscles/*m. soleus* than the thigh muscles/*m. vastus lateralis.* A greater decrease in calf muscle mass was related to a decrease in the expression/deactivation of translation regulators, but not to the expression of the main sarcomeric proteins. At the same time, a significant decrease in aerobic performance of the ankle plantar flexors occurred without changing the expression of oxidative enzymes – a marker of mitochondrial density. That decrease was associated with dysregulation of mitochondrial biogenesis. Most large-scale changes in the transcriptome did not translate into changes in the proteome, suggesting a redundancy in regulation at the mRNA levels. However, changes in the RNA levels were revealed to play a dominant role in regulating specific proteins, whereas for others, this factor played little or no role. In conclusion, our findings partially explain why calf muscles with a strong postural function are more sensitive to short-term disuse. This provides a foundation for developing targeted approaches to counteract the negative effects of disuse on different muscles.

Keywords: disuse, skeletal muscle, transcriptome, proteome, protein expression, translation, mitochondria, heat shock proteins, antioxidant defense.

INTRODUCTION

Disuse lasting more than a week causes a significant decrease in mass and functional capacity of skeletal muscles, including maximum voluntary contraction, aerobic performance, the ability to oxidize fats and carbohydrates, and insulin sensitivity (Marusic et al., 2021; Mikines et al., 1991; Ried-Larsen et al., 2017). A decrease in muscle mass is mainly observed in the trunk postural and leg muscles; moreover, the calf muscles, in particular *m. soleus*, show the greatest decrease (Hardy et al., 2022). This is mainly due to the fact that *m. soleus* has a strong postural function and is composed of more than 80% slow-twitch type I muscle fibers. It means it is much more sensitive to a reduction in contractile activity than other leg muscles (in terms of muscle mass, fiber size, maximum voluntary contraction, and tone) (Borzykh et al., 2025b;

Casuso et al., 2024; Fitts et al., 2010; Kozlovskaya et al., 2007; LeBlanc et al., 1992; Tomilovskaya et al., 2019). The loss of skeletal muscle mass and functional capacity during disuse have been studied for decades, but the mechanisms underlying the specific responses of different muscles to disuse remain unclear.

A key factor regulating the disuse-induced decrease in the mass of human "mixed" skeletal muscles (e.g., *m. vastus lateralis*) is a decrease in translation rate (Brook et al., 2022; Crossland et al., 2019; Deane et al., 2024). However, it is unclear whether this decrease varies between different muscles. Although literature has described the possibility of transcript-specific regulation of individual mRNA translation (Leppek et al., 2018), the disuse-induced decrease in protein synthesis has a generalized effect that appears to suppress the translation of most or all mRNAs. This should lead to a decrease in the absolute amount of most or all proteins in the muscle fibers (and a decrease in muscle mass) without changing proteins concentration. On the other hand, the rate of mRNA translation (and the number of synthesized protein molecules) is regulated by changes in mRNA concentration. Interestingly, after 6 days of disuse, the expression of three times more genes (~1,500 mRNAs) changed in human *m. soleus* than in *m. vastus lateralis* (~600 mRNAs) (Borzykh et al., 2025a; Borzykh et al., 2025b), and this difference persisted after 2 months of disuse (Chopard et al., 2009). It means that disuse may lead to a change in the concentration of more proteins in *m. soleus*, than in *m. vastus lateralis*, and consequently the decreased functional capacity of these muscles might be partially explained by this difference.

In human skeletal muscles, changes in the proteome profile induced by disuse occur more slowly than changes in the transcriptome. Indeed, after 3 days (*m. soleus*) and 6 days (*m. soleus* and *m. vastus lateralis*) of "dry" immersion, no changes were detected (Borzykh et al., 2025b; Popov et al., 2023), whereas after 14 days of limb immobilization, only 99 proteins in *m. vastus lateralis* changed their concentrations (Doering et al., 2022). This is because, *i*) in these studies less than one-third of the skeletal muscle proteome were identified (~2,000 predominantly highly abundant proteins); *ii*) most of highly abundant proteins have a half-life of more than one week, in particular cytoskeletal/sarcomeric proteins, extracellular matrix and mitochondrial proteins, and histones (Fornasiero et al., 2018; Rolfs et al., 2021). The latter suggests that the changes in the concentration of many mRNA occurred in the first days of disuse may lead to changes in the protein concentration and functional capacity of muscles at a later stage. These changes are likely to be more pronounced in *m. soleus* compared to *m. vastus lateralis*.

The aim of the study was: *i*) to compare the changes in the phenotype and proteomic profile of the ankle plantar flexor muscles/*m. soleus* and knee extensors/*m. vastus lateralis* after three weeks of head-down bed rest, and *ii*) to assess the extent to which these proteomic changes

are regulated at the mRNA and other levels. For this purpose, the mass of the thigh and calf muscles, their maximum voluntary contraction, and aerobic performance were measured before and after disuse, and compared to the maximum mitochondrial respiration rate, proteomic (global quantitative mass spectrometry-based proteomic) and transcriptomic (RNA-sequencing) profiles of samples from *m. soleus* and *m. vastus lateralis* (Fig. 1).

METHODS

Ethical approval

The study was approved by the Biomedical Ethics Committee of the Institute for Biomedical Problems of the RAS (Protocols No. 599, October 6, 2021, and No. 621, August 8, 2022) in compliance with the Declaration of Helsinki. All volunteers provided written informed consent for participation and skeletal muscle biopsy.

Study design

Design of the study was described previously (Puchkova et al., 2024). Briefly, 12 healthy men (aged 24–40 years; median height: 1.78 m interquartile range [1.73–1.82 m]; body mass: 78 kg [72–81 kg]; BMI: 23.4 kg/m² [22.3–26.9 kg/m²]) participated in a 21-day head-down (-6 degree) bed rest. Following a familiarization session, muscle performance testing was conducted two days prior to and 8-10 h after the bed rest (after other tests, which were not included in the study) (Fig. 1A). The maximum isometric voluntary contraction (MVC) of the ankle plantar flexors and knee extensors in the right leg was examined. After a 10-minute rest period, aerobic performance of these muscle groups was measured (the maximum power [W_{max}] in an incremental ramp test to exhaustion). Muscle biopsies were obtained using a Bergstrom needle under local anesthesia (2 ml of 2% lidocaine) from the middle part of *m. vastus lateralis* and *m. soleus* 14 days prior to and 20 days following the start of bed rest (Fig. 1A). Biopsies were performed at 10:00 am, three hours after a standardized light breakfast (5.2 g protein, 2.7 g fat, 55 g carbohydrates, 1253 kJ). Samples were processed to remove connective and adipose tissue; part of the fresh tissue was used to assess mitochondrial function; another part was immediately frozen in liquid nitrogen to study the transcriptome and proteome profiles; all frozen samples were stored at -80°C until further analysis.

Lean mass

The lean mass of each leg and calf was assessed using dual-energy X-ray absorptiometry (scan mode "Whole Body", densitometer Hologic, USA). To calculate the thigh lean mass, the calf lean mass was subtracted from the leg lean mass. Mean values for the left and right legs were then calculated.

Muscle performance tests

All testing protocols were described elsewhere (Borzykh et al., 2025b). Briefly, to reduce the contribution of the biarticular gastrocnemius muscles to force production, isometric MVC of plantar flexors was assessed using a CalfRaise-PRO dynamometer (AntexLab, Russia) in a sitting position (knee joint angle was 70 degrees, position of the calf was vertical, and the ankle joint angle was 90 degrees; the distal part of the foot was placed on a 4 cm high stand) (Supporting information Fig. S1). Then, the isometric MVC of the knee extensors was examined in a sitting position at a knee joint angle 110 degrees using a Pro System 3 dynamometer (Biodex, USA). In each test, each participant completed 5 attempts, separated by at least a 30-second rest period; the best one was taken into account.

Maximum aerobic power (W_{max}) of the ankle plantar flexors was assessed using a CalfRaise-PRO ergometer in an incremental ramp test to exhaustion in a sitting position (as described above). The initial load for raising the calf was 30 N, the load increment was 25 N/min; the load during calf lowering was minimal. The subject performed rhythmic (0.5 cycle/s) flexions and extensions of the ankle joint (raising the calf with 55% of the maximum amplitude) until they could no longer maintain the full range of motion for five cycles in the given rhythm.

The W_{max} of the knee extensors was assessed with an incremental ramp test to exhaustion using a modified Ergoselect 900 cycle ergometer (Ergoline, Germany) in a reclining sitting position (hip joint 135 degrees) (Supporting information Fig. S1). Each subject performed rhythmic (1 cycle/s) knee extensions and flexions (from 80 to 160 degrees). The initial load was 0 W, the load increment – 1.1 W/min, and the load during knee flexion was minimal. The test was stopped when the subject was unable to maintain the full amplitude for 5 cycles in the given rhythm.

Mitochondrial respiration in permeabilized muscle fibers

As described previously (Borzykh et al., 2025b), a piece of fresh tissue (~10 mg) was placed in ice-cold BIOPS relaxation buffer (10 mM Ca-EGTA buffer, 0.1 μM free calcium, 20 mM imidazole, 20 mM taurine, 50 mM K-MES, 0.5 mM DTT, 6.56 mM $MgCl_2$, 5.77 mM ATP, 15 mM phosphocreatinine, *pH* 7.1) to remove connective and adipose tissue. Then a small piece

(~2 mg) was removed and the muscle fibers were separated using a pair of needles to create a fiber bundle. The fibers were permeabilized in BIOPS buffer containing saponin (50 μg/ml, 30 min) on ice with slow stirring, then washed twice for 10 minutes in MiRO5 buffer (0.5 mM EGTA, 3 mM $MgCl_2 \cdot 6H_2O$, 60 mM lactobionic acid, 20 mM taurine, 10 mM KH_2PO_4, 20 mM HEPES, 110 mM D-sucrose, 1 g/l fatty acid-free bovine serum albumin). Mitochondrial respiration rate was measured simultaneously on two separate channels using an Oxygraph polarograph (Hansatech, UK) under hyperoxic conditions (Co_2 >200 μM). Substrates were added sequentially: malate (2 mM; final concentration) + pyruvate (5 mM) + glutamate (10 mM), ADP (5 mM) + $MgCl_2$ (3 mM), succinate (10 mM) (to examine maximal ADP-stimulated respiration, state 3), and cytochrome C (10 μM) (to check mitochondrial membrane integrity). The respiration rate without the addition of substrates was subtracted from the respiration rate after the addition of substrates, then the respiration rate was normalized to the mass of permeabilized muscle fibers.

Quantitative mass spectrometry-based proteomics and data processing

As described previously (Kurochkina et al., 2024), a piece of frozen tissue (~10 mg) was homogenized in 140 μl of lysis buffer (4% sodium dodecyl sulfate, 0.1 M Tris and 0.1 M dithiothreitol, *pH* 7.6). The lysate was heated (95ºC, 5 min), transferred to an AFA microtube, sonicated (average power 20 W, 30 s × 4) using a ME220 sonicator (Covaris, USA), and centrifuged (5 min, 30,000 g). The protein concentration in the supernatant was measured by a fluorimeter Qubit 4.

The proteins (85 μg) were diluted in lysis buffer (final volume 24 μl), transferred to an S-Trap column (ProtiFi, USA), alkylated (20 mM iodoacetamide, 15 min), and hydrolyzed into the S-Trap column using trypsin (2 h at 47°C, 1:10, Promega, USA) in 40 μl 50 mM triethylammonium bicarbonate according to the manufacturer's recommendations. After elution, 20 μg of peptides (fluorimeter Qubit 4) were dried, resuspended in 100 mM triethylammonium bicarbonate, and labelled with TMT 16-plex isobaric labels (Thermo Scientific, USA) for 1.5 h according to the manufacturer's recommendations. The reaction was stopped (0.3% hydroxylamine w/v, 15 min), and samples were pooled.

The mixture of labelled peptides was separated using high *pH* reverse-phase LC fractionation (HPLC 1200, Agilent, USA). The peptides were concentrated on an analytical column (XBridge C18, particle size 5 μm, 4.6 x 250 mm, Waters, Ireland) in isocratic mode at a flow of 750 μl/min for 3 min in mobile phase A (15 mM ammonium acetate, *pH* 9.0). Twenty-four fractions were collected from 3 min to 50 min (collection time 2 min, volume 1500 μL) using a gradient elution mode with mobile phase B (15 mM ammonium acetate, *pH* 9.0, 80%

acetonitrile, *pH* 9.0). Each fraction was concentrated, and then fractions (1 and 13, etc.) were combined to obtain 12 resulting fractions.

Each fraction was analyzed two times using an HPLC Ultimate 3000 RSLC nanosystem (Thermo Scientific, USA) and a Q Exactive HF-X Hybrid Quadrupole-Orbitrap mass spectrometer (Thermo Scientific, USA) by the nanoelectrospray ion source in the positive mode of ionization (Thermo Scientific) as previously described. The gradient (60 min) was formed by the mobile phase A (0.1% formic acid) and B (80% acetonitrile, 0.1% formic acid) at a 0.33 μL/min flow. The ionizing voltage was 2.1 kV. MS spectra were acquired at a resolution of 60,000 in the 440–1800 m/z range; fragment ions were mass scanned at a resolution of 60,000 at the range from m/z 120 to the upper m/z value as assigned by the mass to charge state of the precursor ion. All tandem MS scans were performed on ions with a charge state from z=2+ to z=4+. Synchronous precursor selection facilitated the simultaneous isolation of up to 20 MS2 fragment ions. The maximum ion accumulation times were set to 50 ms for precursor ions and 25 ms for fragment ions. AGC targets were set to 10^6 and 10^5 for precursor ions and fragment ions, respectively.

Peptide and protein identification and search were conducted using the MaxQuant platform (version 2.1.4.0; Max Planck Institute for Biochemistry, RRID:SCR_014485) using default settings (FDR for peptides 1%, N-terminal acetylation and oxidation of methionine as variable modifications, and carbamidomethylation of cysteine, as fixed modification) and the *Isobaric much between runs* and *PSM-level weighted ratio normalization* functions (Yu et al., 2020). Further analysis was performed using a Perseus platform (1.6.5; Max Planck Institute for Biochemistry, RRID:SCR_015753). After filtration (potential contaminants, reverse peptides, peptides identified only by site), proteins identified by more than one peptide (unique+razor) and presented in 100% of the samples were selected for further analysis. Reporter ion intensities were log-transformed and normalized to the median. To compare response to disuse in different muscles the 2-way ANOVA (interaction of factors Muscle × Disuse) was used (Perseus platform); *p*-values were adjusted (FDR) using the *p.adjust* package (R environment). The effect of disuse on each muscle was assessed using the two-sample Welch T-test with permutation-based FDR (*q*- or p_{adj}-value; Perseus platform). Differentially expressed proteins were defined using $p_{adj} < 0.05$.

Western blot analysis

As described previously (Borzykh et al., 2025b), the lysate samples were mixed with Laemmli buffer and loaded onto 10% polyacrylamide gels (20 μg protein/lane). Electrophoresis (20 mA per gel) was performed using a Mini-PROTEAN Tetra Cell system (Bio-Rad, USA).

The proteins were transferred to nitrocellulose membranes using a Trans-Blot Turbo system (Bio-Rad) in Towbin buffer for 30 min at 25 V. The membranes were stained with Ponceau S to verify consistent loading of proteins, followed by washing and incubation for 1 h in 5% non-fat dry milk (Sigma-Aldrich, USA) in TBST (150 mM NaCl, 0.1% Tween 20, 20 mM Tris-HCl, *pH* 7.6). Next, the membranes were incubated at 4°C overnight with antibodies: anti-phospho-4EBP1 (Eukaryotic translation initiation factor 4E-binding protein 1) Thr37/46 (1:1000; 236B4; #2855, RRID:AB_560835) or anti-phospho-EF2 (Elongation factor 2) Thr57 (1:1000; #2331, RRID:AB_10015204) (all from Cell Signaling Technology, USA) or anti-phospo-KS6A1 or p90 (Ribosomal protein S6 kinase alpha-1) S380 (1:1000, ab32203, RRID:AB_777767) or anti-G3P or GAPDH (Glyceraldehyde-3-phosphate dehydrogenase; 1:2500, ab9485, RRID:AB_307275) or anti-TBA4A (Tubulin alpha-4A chain; 1:7500, ab176560, RRID:AB_2860019) (all from Abcam, UK) in 5% non-fat dry milk in TBST. Membranes were then incubated for 1 h at room temperature with an anti-rabbit IgG secondary antibody (1:10000, #7074, Cell Signaling Technology, RRID:AB_2099233) in 5% non-fat dry milk in TBST. After each step, the membranes were washed three times for 5 min with TBST. Finally, the membranes were incubated with SuperSignal West Femto Maximum Sensitivity Substrate (Thermo Fisher Scientific, USA) and luminescent signals were captured using a ChemiDoc Imaging System (Bio-Rad). Images were analyzed using the Image Lab Software (v6.0.1, Bio-Rad, RRID:SCR_014210); signals from phosphoproteins were normalized to the mean signal from G3P and TBA4A.

RNA sequencing and data processing

A frozen tissue sample (~15 mg) was homogenized at 4°C in 500 µl of a lysis buffer (LRU-100-50, Biolabmix, Russia) using a plastic pestle and a drill (200 rpm, ~ 30 s). Total RNA (without small RNA fraction) was extracted with phenol-chloroform method and selective sorption on a silicon membrane. RNA concentration was measured with a Qubit 4 fluorometer (ThermoScientific, USA), and RNA integrity was measured using capillary gel electrophoresis (TapeStation, Agilent, USA). The median RNA integrity number (RIN) across all samples was 8.2 (7.9-8.3).

As described previously (Kurochkina et al., 2024), strand-specific RNA libraries were prepared using 500 ng of total RNA, by the NEBNext Ultra II RNA kit (New England Biolabs, USA) in accordance with the manufacturer's instructions. The efficient concentration of the libraries was assessed by qPCR using the 5X qPCRmix-HS SYBR kit (Evrogen, Russia). Single-end sequencing was performed on a NextSeq 550 analyzer (Illumina, USA) with a read length of

75 bp and an average of ~60 million reads per sample. Raw data has been deposited to NCBI GEO: GSE310858.

Sequencing quality was assessed using the *FastQC* tool (v.0.11.5, RRID:SCR_014583), and low-quality reads were removed using *Trimmomatic* (v.0.36, RRID:SCR_011848). High-quality reads were mapped to the human reference genome GRCh38.p13 primary assembly. The number of unique reads mapped to exons of each gene was determined using the *Rsubread* package (R environment) and Ensembl annotation (GRCh38.101). Protein-coding genes (including polymorphic pseudogenes and translated pseudogenes) with TPM >1 (Transcripts Per Million, kallisto tool v0.46.2) were used to analyze differential gene expression by the DESeq2 method using the paired Wald test (with factor Subject) and Benjamini-Hochberg correction. The influence of different muscles on the response to disuse was assessed using a model with interaction of factors (Muscle × Disuse) for paired comparisons (Wald test). Differentially expressed genes were defined as protein-coding genes with p_{adj} <0.01, and magnitude of change ≥25%.

Statistical analysis

Data are presented as the median and interquartile range. A nonparametric Wilcoxon test was used to evaluate the significance of changes following disuse or between different muscle groups, with a significance level set at 0.05. For transcriptomic and proteomic data, a functional enrichment analysis for biological processes, cellular components and pathways (UNIPROT KW BP/CC, GENE ONTOLOGY BP/CC DIRECT and KEGG PATHWAY databases) was performed against all expressed protein-coding genes (TPM >1, ~11,000 mRNA) or detected proteins (~1,900 proteins) using the DAVID tool v2023q4 (RRID:SCR_001881) (Fisher's exact test with Benjamini correction, p_{adj} <0.05). Forward stepwise multiple regression was used to examine the effect of protein half-life and changes in mRNA levels on disuse-induced changes in protein expression; mouse skeletal muscle protein half-life data were taken from (Rolfs et al., 2021).

RESULTS

The functional capacity of calf and thigh muscles

Three weeks of bed rest resulted in a comparable reduction in MVC between the ankle plantar flexors (median 7.7% and interquartile range (5.2 - 10.7)%, p=0.001) and knee extensors (9.4(4.8 - 14.6)%, p=0.002) (Fig. 1, 2B, Supporting Information Fig. S2). However, the decrease in lean mass was greater (p=0.034) in the calf, than in the thigh (6.0(4.0 - 8.0)%, p<0.001 and

4.5(0.2 - 6.7)%, p=0.009, respectively) (Fig. 2C, Supporting Information Fig. S2). In addition, a decrease in maximal aerobic power was only observed in the plantar flexors (12.5(1.1 - 19.4)%, p=0.002); moreover, this response was greater than in the knee extensors (p=0.005) (Fig. 2D, Supporting Information Fig. S2). Meanwhile, the decrease in maximal ADP-stimulated mitochondrial respiration in permeabilized fibers was comparable in *m. soleus* and *m. vastus lateralis* (51(31 - 60)% and 47(23 - 55)%, respectively, both $p \leq 0.001$; Fig. 2E, Supporting Information Fig. S2).

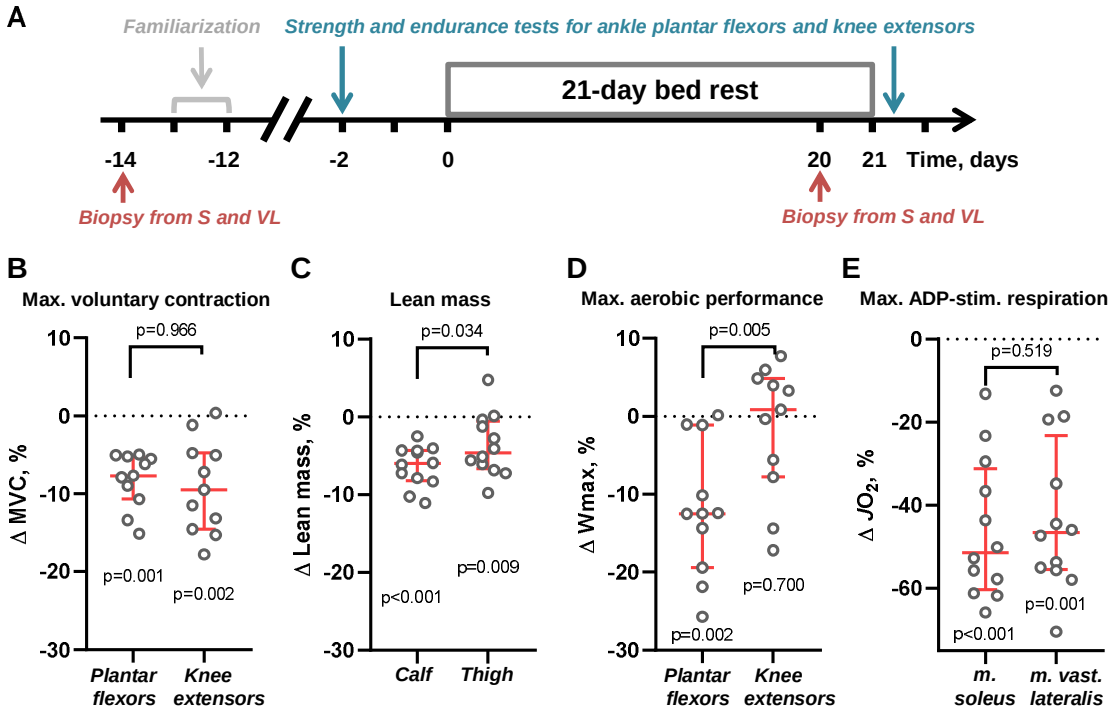

Fig. 1. Three-week bed rest led to more pronounced changes in the phenotype of calf muscles compared to thigh muscles.

(**A**) Study design; *m. soleus* (*S*) and *m. vastus lateralis* (*VL*) (n=12 subjects).

(**B**) Changes in the maximum isometric voluntary contraction of the ankle plantar flexors and knee extensors (n=11 subjects).

(**C**) Changes in calf and thigh lean mass (n=12 subjects).

(**D**) Changes in the maximum power output of the ankle plantar flexors and knee extensors in the incremental ramp test (n=11 subjects).

(**E**) Changes in maximum ADP-stimulated mitochondrial respiration (JO_2) in permeabilized fibers of *m. soleus* and *m. vastus lateralis* (n=12 subjects).

The median and interquartile range. Dotted line – the level prior to disuse. Lower symbols – effect of disuse; upper symbols – differences in response to disuse between muscles (Wilcoxon test).

Proteomic profile in *m. soleus* and *m. vastus lateralis*

Across all samples, 1,844 proteins were identified, predominantly, highly abundant mitochondrial and cytoskeletal/sarcomeric proteins (Supporting Information Fig. S3). Principal component analysis revealed that the differences in proteome between the muscles were more pronounced than the effects of bed rest (Supporting Information Fig. S4A). However, after bed rest, there were significant differences in the number of differentially expressed proteins between the muscles. Specifically, 144 proteins were down-regulated and 126 were up-regulated in *m. soleus*, while only 26 proteins were down- and 16 were up-regulated in *m. vastus lateralis*; these responses significantly overlapped, with only 5 proteins responding only in *m. vastus lateralis* (Fig. 2A, B, Supporting Information Table S1). Proteins that responded in both muscles had a comparable magnitude of expression change. However, for proteins that only responded in *m. soleus*, the magnitude was twice as large as in *m. vastus lateralis* (Supporting Information Fig. S4B). Despite this, no interaction between factors Muscle × Disuse was found (p_{adj} >0.431), apparently due to the large intragroup variation (Fig. 2B).

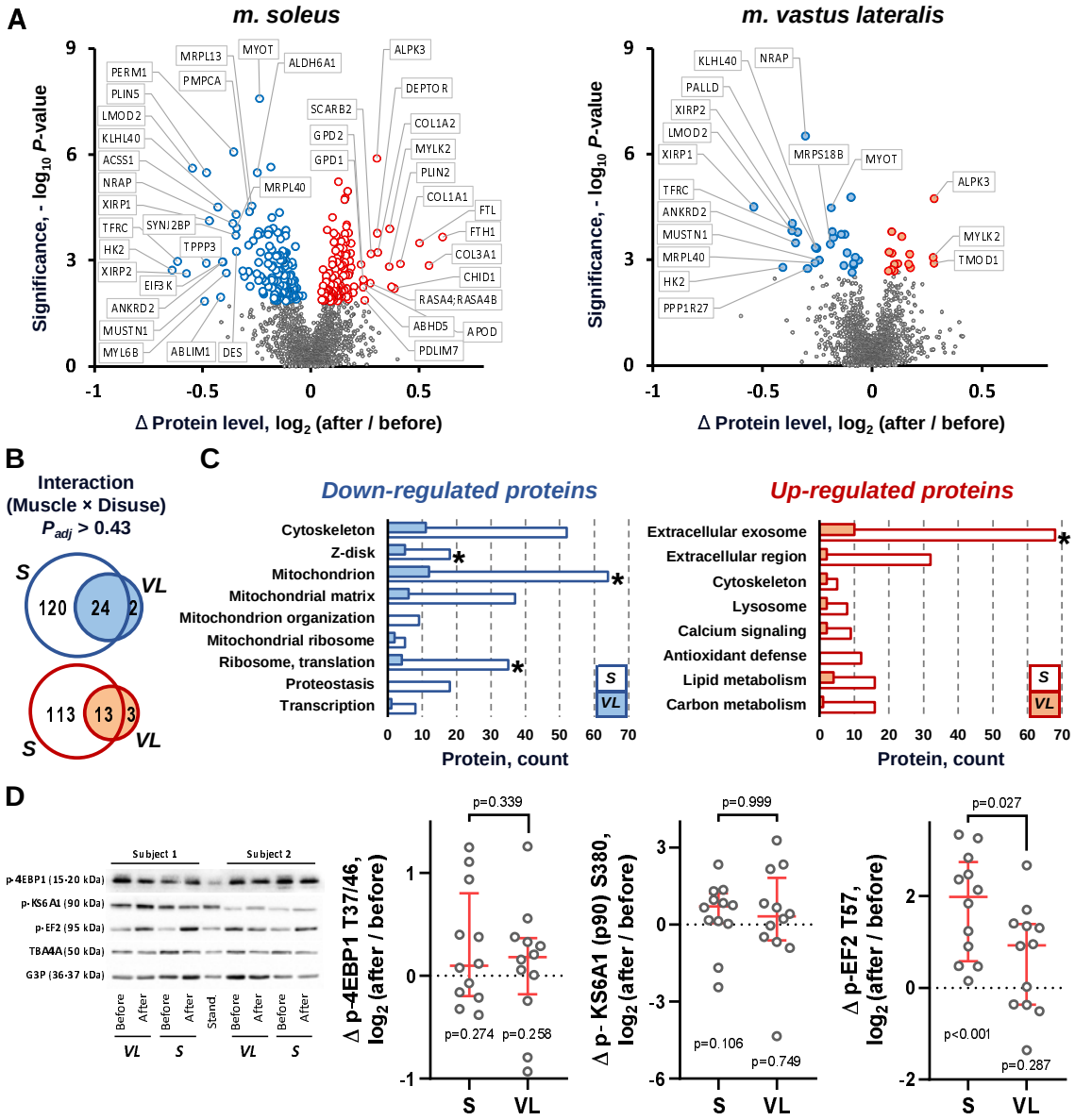

Fig. 2. Three-week bed rest led to greater changes in the proteomic profile in *m. soleus* (*S*) compared to *m. vastus lateralis* (*VL*) (n=11 subjects).

(**A**) The distribution of the expression changes: blue/red points show down- and up-regulated proteins (p_{adj} <0.05), respectively; proteins with a greater response are indicated (see also Supporting Information Table S1).

(**B**) The proteomic response to bed rest, in terms of the number of differentially expressed proteins (p_{adj} <0.05), significantly overlapped between *m. vastus lateralis* and *m. soleus* for both down- and up-regulated proteins.

(**C**) Functional annotation of differentially expressed proteins. Enriched categories are indicated with an asterisk (p_{adj} <0.05; see also Supporting Information Table S1)**.**

(**D**) Changes in the phosphorylation level of canonical sites in translation regulators. The median and interquartile range. Dotted line – the level prior to disuse. Lower symbol – effect of disuse; upper symbol – difference in response to disuse between muscles (Wilcoxon test). *Stand.* – a standard sample, a mixture of six samples of *m. soleus* lysates.

Using UniProt, GO, and KEGG databases, the localization and function of differentially expressed proteins were investigated. In both muscles, bed rest decreased the expression of proteins included in the categories: '*cytoskeleton*', '*Z-disk*', '*mitochondrion*', '*mitochondrial matrix*', '*mitochondrial ribosome*', '*ribosome, translation*', and '*transcription*'; while up-regulated proteins were related to '*extracellular exosomes*', '*extracellular region*', '*cytoskeleton*', '*lysosome*', '*calcium signaling*', '*lipid metabolism*', and '*carbon metabolism*' (Fig. 2C). The response of *m. soleus* was substantially more pronounced in terms of the protein number and included specific categories: '*proteostasis*' and '*mitochondrial organization*' for down-regulated proteins, and '*antioxidant defense*' for up-regulated proteins. Moreover, only *m. soleus* demonstrated significant enrichment for certain categories: '*Z-disk*', '*mitochondrion*', '*ribosome, translation*', and '*extracellular exosome*', for both down- and up-regulated proteins, respectively (Fig. 2C).

Translation regulation in *m. soleus* and *m. vastus lateralis*

Using western blotting, we found no changes in the phosphorylation levels of the canonical sites of Eukaryotic translation initiation factor 4E-binding protein 1 (4EBP1) $^{T37/46}$ and Ribosomal protein S6 kinase alpha-1 (KS6A1 or p90) ^{S380} in both muscles (Fig. 2D). However, in *m. soleus*, a substantial increase in the phosphorylation of another regulator, Elongation factor 2 (EF2) ^{T57} – a marker of its deactivation, was observed ($p<0.001$); moreover, this response was greater than in *m. vastus lateralis* ($p<0.027$) (Fig. 2D).

Transcriptomic profile in *m. soleus* and *m. vastus lateralis*

After removing low-expressed genes, >11,000 mRNAs were identified (Supporting Information Table S2). Principal component analysis revealed that the transcriptomic profile of *m. soleus* was markedly different from that of *m. vastus lateralis* and the disuse-induced changes in the transcriptomic profile of *m. soleus* were substantially greater than those in *m. vastus lateralis* (Supporting Information Fig. S4C). Indeed, 2,018 genes were differentially expressed in *m. soleus*, whereas only 592 – in *m. vastus lateralis*, and most of these (70-80%) overlapped with those found in *m. soleus*. Furthermore, an interaction Muscle × Disuse was found for 920 mRNAs, confirming a stronger response of *m. soleus* to disuse (Fig. 3A; Supporting Information Table S2). Genes that were over-suppressed in *m. soleus* after disuse (relative to *m. vastus*

lateralis) enriched in categories associated with mitochondrial biogenesis (>400 out of ~1000 mRNAs encoding mitochondrial proteins, including most enzymes of the Krebs cycle and oxidative phosphorylation, as well as mitochondrial assembly factors, matrix and membrane proteins). These over-suppressed genes were also associated with regulators of translation, lipid, and amino acid metabolism. Genes that were over-activated in *m. soleus* were related to membrane, extracellular, and cytoskeletal proteins, as well as the immune and inflammatory responses (Fig. 3B-C, Supporting Information Table S2). This finding is consistent with the results of the functional enrichment analysis of genes that respond to disuse in both muscles and in *m. soleus* only (Supporting Information Fig. S5).

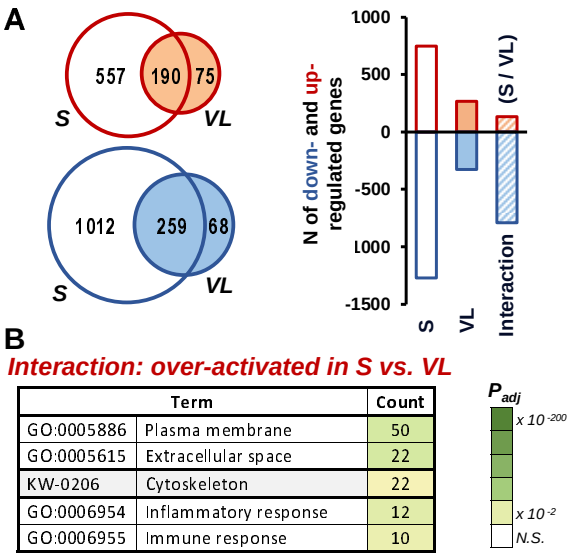

B

Interaction: over-activated in S vs. VL

Term		Count
GO:0005886	Plasma membrane	50
GO:0005615	Extracellular space	22
KW-0206	Cytoskeleton	22
GO:0006954	Inflammatory response	12
GO:0006955	Immune response	10

C

Interaction: over-suppressed in S vs. VL

Term		Count
GO:0005739	Mitochondrion	444
GO:0005743	mitochondrial inner membrane	222
GO:0005759	Mitochondrial matrix	168
hsa00190	Oxidative phosphorylation	76
GO:0032543	Mitochondrial translation	58
GO:0005758	Mitochondrial intermembrane space	36
GO:0005741	Mitochondrial outer membrane	32
GO:0007005	Mitochondrion organization	28
GO:0006099	Tricarboxylic acid cycle	18
GO:0006626	Protein targeting to mitochondrion	16
GO:0006412	Translation	41
hsa03010	Ribosome	31
KW-0443	Lipid metabolism	62
hsa01230	Biosynthesis of amino acids	13
hsa00280	Valine, leucine and isoleucine degradation	27
KW-0576	Peroxisome	20

Fig. 3. Three-week bed rest led to substantially greater changes in the transcriptomic profile of *m. soleus* (*S*) compared to *m. vastus lateralis* (*VL*) in terms of both the number of genes and the magnitude of the response (n=12 subjects).

(**A**) The number of differentially expressed genes (p_{adj} <0.01, |fold change|>1.25) in *m. vastus lateralis* was substantially lower than in *m. soleus*. These down- and up-regulated genes were significantly overlapping. An interaction Muscle × Disuse, confirming a stronger response of *m. soleus* to disuse, was observed for 920 mRNAs.

(**B** and **C**) Functional enrichment analysis of differentially expressed genes that were over-activated or over-suppressed in S after disuse *vs.* VL. Heatmap shows the significance levels, the number – mRNA count (see also Supporting Information Table S2 and Supporting Information Fig. S5).

Comparison of proteomic and transcriptomic responses

To determine how changes in protein expression are regulated at the mRNA levels, we compared the proteomic response to bed rest with changes in the expression of corresponding genes in each muscle and identified distinct patterns of regulation of protein expression at the mRNA levels (Fig. 4A, Supporting Information Table S3). Using multiple regression, we demonstrated that the effect of regulation at the mRNA levels, as well as the protein half-life (data from (Rolfs et al., 2021)), to changes in protein expression differs significantly across different regulatory patterns (Fig. 4B). Functional enrichment analysis revealed that in *m. soleus*, proteins with *'mRNA Down - Protein Down'* regulation pattern were enriched in categories related to various mitochondrial proteins, particularly mitochondrial matrix proteins; those included regulator of mitochondrial biogenesis and proteostasis, but were not related to the Krebs cycle or oxidative phosphorylation (Fig. 4C, Supporting Information Table S3). Meanwhile, proteins with the regulation pattern *'mRNA NS - Protein Down'* enriched in categories related to cytoplasmic proteins, including ribosomal and cytoskeletal (Z-disk) proteins, as well as regulators of focal adhesion, myogenesis, and differentiation. On the other hand, up-regulated proteins, showing no correlation with changes in their mRNAs (patterns *'mRNA NS - Protein Up'* and *'mRNA Down - Protein Up'*), enriched in other categories, such as *'extracellular exosome'* and *'lipid metabolism'*. No significant enrichment was observed for *m. vastus lateralis*, due to the smaller number of differentially expressed proteins.

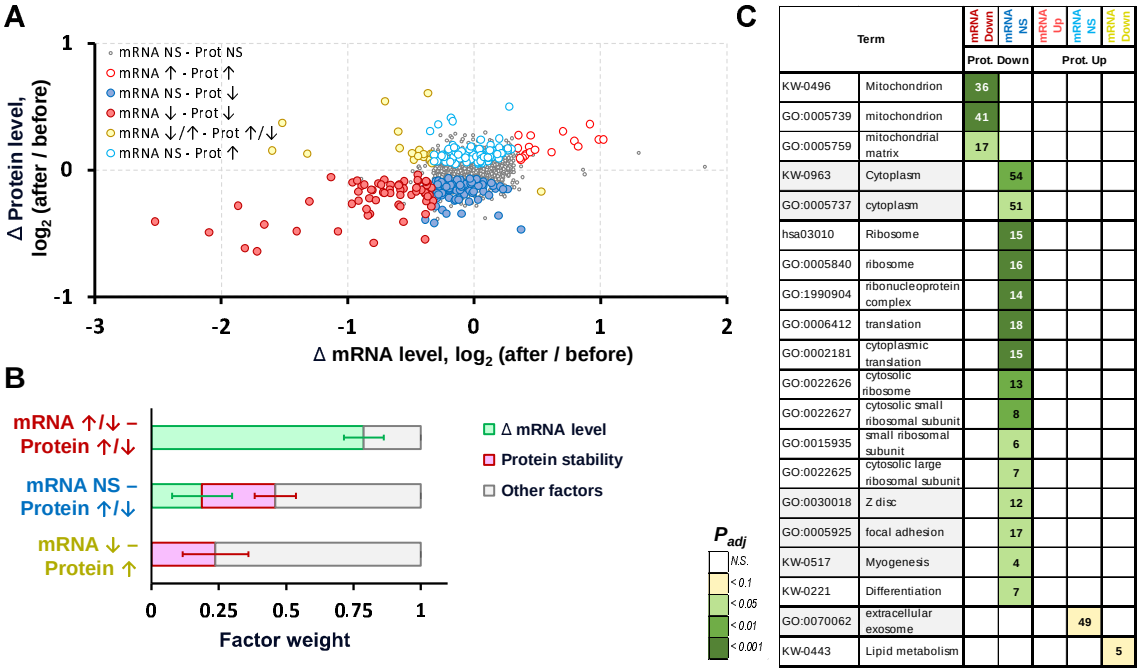

Term		mRNA Down	mRNA NS	mRNA Up	mRNA NS	mRNA Down
		Prot. Down		Prot. Up		
KW-0496	Mitochondrion	36				
GO:0005739	mitochondrion	41				
GO:0005759	mitochondrial matrix	17				
KW-0963	Cytoplasm		54			
GO:0005737	cytoplasm		51			
hsa03010	Ribosome		15			
GO:0005840	ribosome		16			
GO:1990904	ribonucleoprotein complex		14			
GO:0006412	translation		18			
GO:0002181	cytoplasmic translation		15			
GO:0022626	cytosolic ribosome		13			
GO:0022627	cytosolic small ribosomal subunit		8			
GO:0015935	small ribosomal subunit		6			
GO:0022625	cytosolic large ribosomal subunit		7			
GO:0030018	Z disc		12			
GO:0005925	focal adhesion		17			
KW-0517	Myogenesis		4			
KW-0221	Differentiation		7			
GO:0070062	extracellular exosome				49	
KW-0443	Lipid metabolism					5

Fig. 4. Patterns of protein regulation depend on their function.

(**A**) Bed rest-induced changes in protein expression and the levels of corresponding mRNAs in *m. soleus* (each point depicts the median, different colors indicate different regulation patterns; *NS* – non significant).

(**B**) The effect of changes in the mRNA levels and protein half-life on disuse-induced changes in protein expression for different regulatory patterns.

(**C**) Functional enrichment analysis of proteins with different regulation patterns in *m. soleus*. The heatmap shows the significance levels, the number – mRNA number in enriched categories (see also Supporting Information Table S3). No enrichment for *m. vastus lateralis* was found.

Interestingly, in *m. soleus*, the transcriptomic analysis revealed substantial amounts of down-regulated mRNAs encoding most of glycolytic, Krebs cycle, and oxidative phosphorylation enzymes as well as some regulators of lipid metabolism and muscle contraction (Supporting Information Fig. S5B). Although most of these proteins were identified by proteomic analysis, no changes in their expression were found (Supporting Information Fig. S6).

DISCUSSION

Three-week bed rest induced more pronounced changes in the phenotype of calf muscles compared to thigh muscles

Our study was the first to comprehensively compare the effects of short-term disuse (3 weeks) on the phenotype, proteome, and transcriptome of calf and thigh muscles. As expected, disuse led to a more pronounced decrease in lean mass in the calf (Marusic et al., 2021). Furthermore, a more pronounced reduction in aerobic performance was found in the ankle plantar flexor muscles compared to the thigh muscles (Fig. 2, Supporting Information Fig. S2). This supports the concept that muscles involved in maintaining posture (gravitationally dependent muscles) are more sensitive to reduced contractile activity (Borzykh et al., 2025b; Fitts et al., 2010; Kozlovskaya et al., 2007; LeBlanc et al., 1992; Tomilovskaya et al., 2019). Despite the absence of a decrease in the aerobic performance of the knee extensors, the maximum ADP-stimulated mitochondrial respiration in permeabilized fibers of *m. vastus lateralis* muscle decreased, and this decrease was comparable to that of *m. soleus*. Disuse did not cause changes in the expression of several dozen detected mitochondrial respiratory enzymes in both muscles (Supporting Information Fig. S6, Supporting Information Table S1). This indicates a decrease in the intrinsic maximum ADP-stimulated mitochondrial respiration, apparently due

to a dysregulation of mitochondrial respiration, which is consistent with the results of experiments with disuse of shorter duration (Borzykh et al., 2025b; Miotto et al., 2019; Popov et al., 2023).

Potential mechanisms for a more significant change in the phenotype of *m. soleus*/ankle plantar flexors compared to *m. vastus lateralis*/knee extensors

Mass spectrometry-based proteomics enables the detection of predominantly highly abundant skeletal muscle proteins, such as sarcomeric, mitochondrial and ribosomal proteins, and chaperons; the coverage of low-abundant regulatory proteins is limited (Supporting Information Fig. S3). Our data, together with the results of other studies (3-, 6-, and 14-day disuse (Borzykh et al., 2025b; Doering et al., 2022; Popov et al., 2023) show that, in contrast to the transcriptome, changes in the expression of highly abundant proteins occur only after 2-3 weeks of disuse. The changes in the proteomic profile were significantly more extensive in "slow" *m. soleus*, in terms of the number of differentially expressed proteins, than in "mixed" *m. vastus lateralis*. This may explain, at least in part, the large difference in phenotype changes between calf and thigh muscles.

Cytoskeletal and extracellular matrix proteins and regulators of protein synthesis

Despite the decrease in lean (muscle) mass of the calf and thigh, no decrease in the concentration of the main sarcomeric proteins was detected in both muscles (isoforms of myosin heavy chains encoded by *MYH1/2/7*, actin, tropomyosin, titin, nebulin, etc.). These proteins have the highest intensity of mass spectrometric peaks (10 out of top 15 proteins) (Supporting Information Fig. S7, Supporting Information Table S1), i.e., they constitute the largest mass portion of muscle proteins. Sarcomeric proteins with decreased expression in both muscles (encoded by *OBSCN*, *MYOT*, *PALLD*, *LMOD2*) or only in *m. soleus* (an unspecific for human skeletal muscle isoform of the myosin heavy chain, encoded by *MYH14*, as well as other sarcomeric proteins: *DES*, *MYOM1*, *MYL6B*/*12A*/*12B*/*18A*, *FLNB*/*C*, *ABLIM1*, *NEXN*, *LMOD3*) had a concentration two orders of magnitude lower than the main sarcomeric proteins (Supporting Information Fig. S7, Supporting Information Table S1). Therefore, the decrease in their expression does not explain the decrease in muscle mass and/or the greater decrease in mass in the calf muscles. However, the decrease in the expression of some Z-disk proteins found in both muscles (Supporting Information Fig. S7, Supporting Information Table S1) may be associated with a decrease in sarcomere transverse stiffness and partially explain the decrease in MVC in both muscle groups (Ogneva et al., 2009).

A decrease in lean (muscle) mass of the calf and thigh, occurring without a change in the concentration of the main sarcomeric proteins, indicates a proportional decrease in their absolute content, which is apparently associated with a decrease in the rate of protein synthesis on ribosomes – the main mechanism for the decrease in the mass of "mixed" human muscle during short-term disuse (Brook et al., 2022; Crossland et al., 2019; Deane et al., 2024). The greater decrease in lean mass in the calf muscles, compared to the thigh muscles, may be explained by a more pronounced decrease in the rate of protein synthesis. This is indirectly confirmed by our data on the increase in *m. soleus*, in contrast to *m. vastus lateralis*, of the phosphorylation level of the key elongation regulator EF2 ^{T57} – a marker of its deactivation (Fig. 2D, Supporting Information Fig. S8). Additionally, in *m. soleus* there was a decrease in the expression of several subunits of translation initiation factors (encoded by *EIF3A/3J/3K/4B* genes) and four dozen ribosomal proteins (including mitochondrial ribosomal proteins) – a marker of a decrease in ribosome content (Fig. 2D, Supporting Information Table S1).

Interestingly, an increase in the expression of some cytoskeletal and extracellular matrix proteins was observed only in *m. soleus*, such as collagens (encoded by *COL1A1/1A2/3A1/15A1*), laminins (*LAMA2/B1*), sarcoglycan *SGCA*, and dystrophin (Supporting Information Fig. S7, Supporting Information Table S1). Fibrillar collagens types I and III – proteins that make up half of the extracellular matrix proteins (McKee et al., 2019) – demonstrated some of the largest amplitudes of expression changes (increases of 1.24- to 1.53-fold). These changes in *m. soleus* are reminiscent of the increased collagen expression, which leads to fibrotic changes in skeletal muscle in various pathological conditions (Agarwal et al., 2025; Mann et al., 2011; McKee et al., 2019). In addition, an increase in the expression of some proteins of the dystroglycan complex has already been noted after 84 days of disuse, both in *m. soleus* and in *m. vastus lateralis* (Chopard et al., 2005). Our results show that in *m. soleus* these changes occur significantly earlier, indicating greater sensitivity of this muscle to disuse. The increased expression of key extracellular matrix proteins that occurs during muscle fiber atrophy should lead to an increase in the proportion of connective tissue in *m. soleus* and musculotendinous stiffness of the ankle plantar flexor muscles. This is confirmed by changes observed during longer-term conditions such as 60-day disuse (Thot et al., 2021) and space flight lasting 90 to 180 days (Lambertz et al., 2001), as well as age-related changes (Pavan et al., 2020).

Proteostasis regulators

It has previously been shown that disuse alters phosphorylation/reduces expression of individual heat shock proteins (encoded by *Hspb1* [small heat shock protein] and *Hspa1a/b*

[HSP70 family]), as well as the transcription factor HSF1 in skeletal muscle of rodents (Lawler et al., 2006; Senf, 2013) and humans (*HSPA9* [HSP70 family]) (Gram et al., 2014). We found that, in contrast to *m. vastus lateralis*, there was a large-scale decrease in the expression of heat shock proteins and their regulators in *m. soleus* (23% or 18 of 79 detected proteins) (Fig. 2C, Supporting Information Table S1). These proteins were localized both in the cytoplasm (e.g., those associated with families of the small heat shock protein [encoded by *CRYAB*], HSP40 [*DNAJA4*/*B4*], HSP70 [*HSPH1*, *BAG2*/*3*], and HSP90 [*HSP90AA1*/*AB1*, *AHSA1*], as well as *PFDN2*/4) and in mitochondria (e.g., those associated with the HSP10 [*HSPE1*], HSP60 [*HSPD1*], HSP70 [*HSPA9*], HSP90 [*HSP90AA1*/*AB1*, *TRAP1*], and *PFDN2*/*4* families). Studies with overexpression of *Hspb1*, *Hspa1a*/*b*, and *Hspe1* have shown that chaperones play a significant role in preventing the decline in muscle mass and strength caused by disuse and certain pathological conditions. This is likely due to the fact that various chaperones are able to maintain the structure and stability of key sarcomeric proteins, preventing their aggregation, and can also influence the regulation of proteolysis and myogenesis (see review (Pomella et al., 2023)). More than 99% of mitochondrial proteins are encoded by the nuclear genome and synthesized in the cytoplasm; therefore, cytoplasmic and mitochondrial chaperones play a key role in the transport and import of these proteins into mitochondria. A decrease in muscle contractile activity caused by denervation reduces the import of mitochondrial proteins; this correlates with impaired mitochondrial respiration and the production of reactive oxygen species, which occurs along with decreased mitochondrial HSP70 (*Hspa9*) expression (Singh and Hood, 2011). This is consistent with our data on the decrease in the expression of the chaperone HSPA9, mitochondrial peptidases PMPCA/B, which cleave imported precursor proteins, and the component of the inner membrane translocase TIMM50 in *m. soleus* (Supporting Information Table S1). Together, these data suggest that, in our study, the larger reduction in chaperone concentrations in *m. soleus* may partially explain the more pronounced reduction in calf muscle mass and aerobic performance.

Mitochondrial proteins

Surprisingly, no reduction in the concentration of oxidative phosphorylation enzymes, which constitute about a third of human mitochondrial proteins (Morgenstern et al., 2021) and are markers of mitochondrial density, was detected in *m. soleus* (Supporting Information Fig. S6). The literature presents mixed data on changes in mitochondrial density after 2-3 weeks of disuse (see review (Delfinis et al., 2025)). However, with longer-term disuse (30-64 days), there is a decrease in mitochondrial density observed in *m. soleus*, either greater (Hikida et al., 1989; Trappe et al., 2024) or comparable (Hendrickse et al., 2022) in amplitude to that of *m. vastus*

lateralis. Taken together, these findings suggest that in human skeletal muscle, disuse-induced declines in mitochondrial function occur in two stages. During the first few weeks, there is mitochondrial dysregulation, followed by a reduction in the content of respiratory enzymes and mitochondria during the second stage; moreover, *m. soleus* shows a more rapid rate of these changes compared to other muscles. Our proteomic data suggest that the dysregulation occurring in the first stage are caused by complex changes in the expression of proteins regulating proteostasis (as discussed above), mitochondrial biogenesis, oxidative stress, and calcium homeostasis (see below).

Indeed, only in *m. soleus* did disuse cause a decrease in the expression of several key regulators of mitochondrial biogenesis that regulate mitochondrial fusion and the formation of the mitochondrial reticulum (encoded by *MFN2* and *OPA1*), cristae morphology, and the assembly and functioning of respiratory complexes (*OPA1*, *COA3*, *TMEM11*, and *LONP1*), and degradation of misfolded, unassembled, or oxidatively damaged polypeptides in the matrix (*LONP1*) (Supporting Information Table S1). A number of studies have examined the effect of disuse on the expression of mitochondrial biogenesis regulators in "mixed" human skeletal muscles, but only a few of them have shown a decrease in the expression of MFN2 (Franchi et al., 2025), OPA1 (Noone et al., 2025), and LONP1 (Xu et al., 2022). As revealed our study, the decrease in the expression of mitochondrial biogenesis regulators in "slow" *m. soleus* highlights the greater sensitivity of this muscle to disuse compared to "mixed" *m. vastus lateralis*.

Oxidative stress regulators

Disuse may induce oxidative stress in human skeletal muscle, causing an increase in the expression of antioxidant defense proteins (see review (Delfinis et al., 2025)). Our study revealed an increase in the expression of antioxidant defense proteins only in *m. soleus*: superoxide dismutase 1 – one of the key antioxidant defense enzymes, and other enzymes encoded by *TXN*, *GSTM2*/*P1*, *PARK7*, *PRXL2A*, etc. (Supporting Information Table S1). In addition, we observed a decrease in the expression of proteins related to the complex 'hexokinase 2–mitochondrial non-selective channel porin 1' (HK2-VDAC1), which is involved in the regulation of mitochondrial reactive oxygen species production (Vyssokikh et al., 2020) and the permeability of the mitochondrial outer membrane to ions and small molecules (Chiara et al., 2008). Interestingly, HK2 showed the largest magnitude of expression reduction in *m. soleus* (1.56-fold) and one of the largest in *m. vastus lateralis* (1.33-fold), whereas a decrease in VDAC1 expression was detected only in *m. soleus* (1.06-fold) (Fig. 2, Supporting Information Table S1). Taken together, these results indirectly indicate oxidative stress in *m. soleus*, which

may be one of the reasons for the impaired mitochondrial function in this muscle and the decrease in aerobic performance of the ankle plantar flexors.

Calcium homeostasis regulators

Similar to the changes described above, increased expression of calcium homeostasis regulators was found primarily in *m. soleus* (Fig. 2C, Supporting Information Table S1). Disuse disrupts calcium homeostasis in muscle fibers, increasing the level of calcium ions in the cytoplasm and mitochondria (Michelucci et al., 2021). Therefore, in *m. soleus*, the disuse-induced increase in expression of key regulators of calcium translocation to and binding into the sarcoplasmic reticulum (encoded by *ATP2A2* [slow-twitch fiber isoform *SERCA2*] and *CASQ1*) and the decrease in expression of calcium transporters to mitochondria (encoded by *VDAC* and *MCU*) may be aimed at normalizing the elevated levels of cytoplasmic and mitochondrial calcium, respectively. Unexpectedly, disuse also increased the expression of key regulators of calcium ion release from the sarcoplasmic reticulum: Ryanodine Receptor 1 and Triadin (encoded by *RYR1* and *TRDN*), which is consistent with the increase in RYR1 expression in human *m. soleus* after ~180-day spaceflight (Blottner et al., 2023). The increase in the level of these proteins may partially explain the disuse-induced (and oxidative stress-related) increase in calcium ion leakage into the cytoplasm, leading to the activation of calcium-dependent proteolysis and mitochondrial dysfunction (Michelucci et al., 2021). Our data indicate a disruption in the regulation of calcium homeostasis occurring predominantly in *m. soleus*, which may partially explain the greater decrease in calf muscle mass and ankle plantar flexor performance than in the thigh muscles.

Patterns of protein regulation depend on their function

The most significant changes in the transcriptome of *m. soleus* that occur from the first days of disuse are the suppression of genes encoding regulators of energy metabolism, in particular mitochondrial oxidative enzymes (Fig. 3, Supporting Information Fig. S5 and (Borzykh et al., 2025b; Popov et al., 2023)). However, even after 3 weeks of disuse, most large-scale changes in the transcriptome did not translate into changes at the protein levels, for example, oxidative phosphorylation and the Krebs cycle enzymes, as well as glycolytic enzymes, regulators of lipid metabolism and muscle contraction (Supporting Information Fig. S6). This may be explained by the long half-life of these proteins (Fornasiero et al., 2018; Rolfs et al., 2021) and/or the insufficient duration of disuse. On the other hand, it indicates redundancy of regulation at the mRNA levels and, consequently, the priority of translation and/or proteolysis in

regulating the decrease in absolute protein content (and muscle mass) during short-term disuse. The latter is consistent with studies that have investigated the decrease in protein synthesis rate in "mixed" human skeletal muscle during disuse (Brook et al., 2022; Crossland et al., 2019; Deane et al., 2024) and with our findings of a marked increase in EF2 ^{T57} phosphorylation levels, a decrease in expression of several translation initiation factors, and ribosomal proteins in *m. soleus* (Fig. 2D, Supporting Information Table S1).

Transcriptomic and proteomic studies have shown that the level of mRNA is a poor predictor of protein expression (Buccitelli and Selbach, 2020; Liu et al., 2016). However, when analyzing proteins that changed expression in *m. soleus*, we found that regulation at mRNA levels played a dominant role (factor weight = 0.79) in changing the expression of some proteins (regulation pattern '*mRNA Down - Protein Down*' or '*mRNA Up - Protein Up*'), while for others, this factor played little (factor weight = 0.19 for regulation pattern '*mRNA NS - Protein Down*' and '*mRNA NS - Protein Up*') or no role (regulation pattern '*mRNA Down - Protein Up*') (Fig. 4B). Moreover, for the latter two cases, protein stability and unknown variables (apparently, the rate of protein synthesis) played an important role in protein regulation. Importantly, our data shows that patterns of protein regulation depend on their function. Proteins from the '*mRNA Down - Protein Down*' group were enriched in functional categories associated with mitochondria. This group included key regulators of mitochondrial dynamics and structure (encoded by *MFN2*, *OPA1*, as well as *COA3*, *NDUFAF4*, and *TMEM11*), and a number of chaperones that play a key role in the transport, import, and folding of mitochondrial proteins (encoded by *HSP90AA1*, *HSPA9*, *HSPE1*, *HSPD1*, and *CRYAB*) (Supporting Information Table S3). In addition, for other regulatory patterns that we identified, examples of coregulation of genes with similar or complementary functions were also found: ribosomal and sarcomeric proteins were enriched in the '*mRNA NS - Protein Down*' group, proteins that are part of exosomes – in the '*mRNA NS - Protein Up*' group, and regulators of lipid metabolism – in the '*mRNA Down - Protein Up*' group, (Fig. 4C). Coregulation of the expression of genes with similar or complementary functions is well known, including human skeletal muscle during disuse (Borzykh et al., 2025a). Our data show that proteins with similar or complementary functions may have a specific pattern of regulation at the mRNA and other levels of regulation. This observation is consistent with studies comparing changes in protein and mRNA expression in human skeletal muscle after chronic aerobic exercise training (Makhnovskii et al., 2020), as well as protein and mRNA stability in cells (Schwanhausser et al., 2011).

Conclusions

Our study was the first to compare the effects of short-term (3 weeks) disuse on the phenotype, proteome, and transcriptome of the calf and thigh muscles. Disuse resulted in a greater decrease in lean mass, aerobic performance, and changes in the proteomic and transcriptomic profiles of the calf muscles/*m. soleus* than the thigh muscles/*m. vastus lateralis*. These results indicate a greater sensitivity of the calf muscles, which have a strong postural function (gravity-dependent muscles), to a decrease in contractile activity. A greater loss in calf muscle mass was related to a decrease in the expression/deactivation of translation regulators in *m. soleus*, but not to the expression of the main sarcomeric proteins. At the same time, a significant decrease in aerobic performance of the ankle plantar flexors occurred without changing the expression of oxidative enzymes – a marker of mitochondrial density – in *m. soleus*. However, that decrease was associated with mitochondrial dysregulation. Our data suggest that this disorder is closely associated with changes in the expression of proteins that regulate the dynamics and structure of mitochondria, cellular and mitochondrial proteostasis, antioxidant defense, and calcium homeostasis.

Comparison of transcriptomic and proteomic data revealed that most large-scale changes in the transcriptome were not translated into changes at the protein levels. It may be due to the long half-lives of the detected proteins (predominantly highly abundant) or insufficient disuse time, and indicates redundancy in regulation at the mRNA levels. On the other hand, it turned out that the pattern of regulation of proteins that changed expression depends on their function. Disuse-induced changes in the RNA levels played a dominant role in regulating expression of some proteins (such as mitochondrial biogenesis regulators), whereas for others (proteins of ribosome and exosome, etc.), this factor played little or no role. Identification of the mechanisms of this gene expression coregulation during disuse and the factors that determine the specific response of different skeletal muscles provides a foundation for developing targeted approaches to counteract the negative effects of disuse on different muscles.

Data availability

Raw transcriptomic data has been deposited to NCBI GEO: GSE310858. Proteomic data are available in Supplementary Table S1.

Competing interests

The authors declare that they have no competing interests/conflicts of interest.

Authors' contributions

A.V.S., D.V.P – concept and supervision of the work; R.Y.Z., T.F.V., E.M.L., A.A.P., G.V.G., V.E.N., A.V.S., D.V.P – work with volunteers and patients, interventions; N.S.K., A.A.B., D.V.P – sample preparation and RNA-seq; M.A.O., D.V.P – sample preparation for mass spectrometry-based analysis; N.E.V., V.G.Z. – samples fractionation and mass spectrometry-based analysis; A.A.B. – western blot analysis; M.A.O., N.S.K., P.A.M., D.V.P. – bioinformatics and statistical data analysis; M.A.O., N.S.K., R.Y.Z., A.A.B., P.A.M., D.V.P. – discussion of the study results and their biological interpretation; M.A.O., N.S.K., D.V.P. – writing the article. All authors approved the final version of the manuscript; agree to be accountable for all aspects of the work in ensuring that questions related to the accuracy or integrity of any part of the work are appropriately investigated and resolved. All persons designated as authors qualify for authorship, and all those who qualify for authorship are listed.

Funding

The work was supported by the Russian scientific foundation (grant # 25-75-20005).

Acknowledgments

Mass spectrometry-based proteomic analysis was performed on the equipment of the “Human Proteome” Core Facility in Institute of Biomedical Chemistry (Moscow).

Supporting Information

Supporting Information Fig. S1. Subject position during a maximal voluntary contraction test for ankle plantar flexors (**A**) and knee extensors (**B**) and during an incremental ramp test to exhaustion for ankle plantar flexors (**C**) and knee extensors (**D**).

Supporting Information Fig. S2. Three-week bed rest induced more pronounced changes in phenotype of calf muscles compared to thigh muscles.

(**A**) Maximum isometric voluntary contraction of the ankle plantar flexors and knee extensors (n=11 subjects).

(**B**) Lean mass of calf and thigh (n=12 subjects).

(**C**) Maximum power of the ankle plantar flexors and knee extensors in the incremental ramp test (n=11 subjects).

(**D**) Maximum ADP-stimulated mitochondrial respiration (JO_2) in permeabilized fibers of *m. soleus* and *m. vastus lateralis* (n=12 subjects).

Median and interquartile range; Wilcoxon test.

Supporting Information Fig. S3. Global mass spectrometry-based proteomics has allowed to detect predominantly highly abundant muscle proteins.

Number of detected proteins related to different protein classes, and the total number of proteins in each protein class, according to the Panther database.

Supporting Information Fig. S4.

(**A**) Principal component analysis of proteomic (n=11 subjects) data. Crosses – *m. soleus*; circles – *m. vastus lateralis*. Black and red – prior to, and after 3-week bed rest, respectively.

(**B**) Regression line of protein expression changes in *m. vastus lateralis vs. m. soleus*: proteins that changed expression (p_{adj} <0.05) in both muscles (above) and in *m. soleus* only (below). Each point is the median expression; the red line is the line of identity.

(**C**) Principal component analysis of transcriptomic (n=12 subjects) data. Crosses – *m. soleus*; circles – *m. vastus lateralis*. Black and red – prior to, and after 3-week bed rest, respectively.

Supporting Information Fig. S5. Three-week bed rest induced substantially greater changes in the transcriptomic profile in terms of differentially expressed gene number in *m. soleus* (*S*) than in *m. vastus lateralis* (*VL*) (n=12 subjects).

(**A**) Transcriptomic response to bed rest in *m. vastus lateralis* overlapped that in *m. soleus*. The number of down- and up-regulated mRNAs (p_{adj} <0.01, |fold change| >1.25) is shown.

(**B**) Functional enrichment analysis of differentially expressed genes overlapping between the muscles and changing expression only in *m. soleus*. The genes that responded in both muscles were associated primarily with down-regulated genes encoding mitochondrial, cytoskeletal/sarcomeric proteins, and regulators of lipid metabolism. The genes that responded only in *m. soleus* were much greater; they were also associated primarily with a decrease in the expression of genes encoding various mitochondrial proteins (>400 out of ~1000 mRNAs encoding mitochondrial proteins, including most Krebs cycle and oxidative phosphorylation enzymes), as well as regulators of carbohydrate and lipid metabolism, ribosomal, and cytoskeletal/sarcomeric proteins. Genes up-regulated only in *m. soleus* were associated with immune and inflammatory response (including the JAK-STAT pathway), calcium signaling, and various chromatin-associated proteins.

Heatmap shows significance levels, number – mRNA count in enriched categories (see also Supporting Information Table S2).

Supporting Information Fig. S6.

Highly expressed down-regulated genes in *m. soleus*, which enriched functional categories related to glycolytic (**A**), Krebs cycle (**B**), and oxidative phosphorylation (**C**) enzymes, as well as some regulators of lipid metabolism (**D**) and muscle contraction (**F**) (see Fig. 3C), demonstrated actually no decrease in expression of corresponding proteins after 3-week bed rest.

Grey bars – mRNAs, black bars – proteins. All grey bars indicate differentially expressed mRNAs (p_{adj} <0.01). Differentially expressed proteins are indicated by asterisks (p_{adj} <0.05).

Supporting Information Fig. S7. Changes in expression of cytoskeletal and extracellular matrix proteins in *m. soleus* (**A**) and *m. vastus lateralis* (**B**) after 3-week bed rest (n=11 subjects). White - non detected (N.D.) proteins, green – not significantly changed (N.S.) proteins, blue and red – down- and up-regulated proteins, respectively (p_{adj} < 0.05). (**C**) Intensity of MS signal for all detected proteins. Black – sarcomeric proteins with unchanged expression, light and dark blue – down-regulated sarcomeric proteins only in *m. soleus* and in both muscles, respectively (p_{adj} < 0.05).

Supporting Information Fig. S8. Original membranes with Ponceau S staining and blots (Western blot analysis).

VL – *m. vastus lateralis,* **S** – *m. soleus,* **b** and **a** – before and after disuse, respectively; **Stand.** – a standard sample, a mixture of six samples of *m. soleus* lysates. **№** – a number of membrane.

Supporting Information Table S1. All detected and differentially expressed proteins (DEPs) after 3-week bed rest in *m. soleus* (*S*) and *m. vastus lateralis* (*VL*), and functional annotation of DEPs. P_{adj} for enriched functional categories is indicated.

Supporting Information Table S2. All detected and differentially expressed protein-coding genes (DEGs) after 3-week bed rest in *m. soleus* (*S*) and in *m. vastus lateralis* (*VL*), DEGs showing an interaction Muscle x Disuse, and result of functional enrichment analysis for interacting DEGs, overlapping (common) DEGs in both muscles and DEGs that responded only in *S*.

Supporting Information Table S3. Comparison of changes, induced by 3-week bed rest, in expression of proteins and corresponding mRNAs in *m. soleus* (*S*) and in *m. vastus lateralis* (*VL*), and result of functional enrichment analysis for proteins showing different regulation patterns in *m. soleus*. DEPs and DEGs – differentially expressed proteins and genes, respectively.

References

Agarwal, V., Gupta, A., Chaudhary, R., and Kumar, A. (2025). Elucidating the potential mechanism and therapeutic targets of chronic stress-induced muscle atrophy. Int Immunopharmacol *162*, 115118.

Blottner, D., Moriggi, M., Trautmann, G., Hastermann, M., Capitanio, D., Torretta, E., Block, K., Rittweger, J., Limper, U., Gelfi, C., et al. (2023). Space Omics and Tissue Response in Astronaut Skeletal Muscle after Short and Long Duration Missions. Int J Mol Sci *24*.

Borzykh, A.A., Makhnovskii, P.A., Ponomarev, II, Vepkhvadze, T.F., Lednev, E.M., Rukavishnikov, I.V., Orlov, O.I., Tomilovskaya, E.S., and Popov, D.V. (2025a). Transcription factors associated with regulation of transcriptome in human thigh and calf muscles at baseline and after six days of disuse. Biochim Biophys Acta Gene Regul Mech *1868*, 195086.

Borzykh, A.A., Zhedyaev, R.Y., Ponomarev, II, Vepkhvadze, T.F., Zgoda, V.G., Orlova, M.A., Vavilov, N.E., Shishkin, N.V., Lednev, E.M., Makhnovskii, P.A., et al. (2025b). Multidirectional effect of low-intensity neuromuscular electrical stimulation on gene expression and phenotype in thigh and calf muscles after one week of disuse. Eur J Appl Physiol *125*, 2431-2447.

Brook, M.S., Stokes, T., Gorissen, S.H.M., Bass, J.J., McGlory, C., Cegielski, J., Wilkinson, D.J., Phillips, B.E., Smith, K., Phillips, S.M., et al. (2022). Declines in muscle protein synthesis account for short-term muscle disuse atrophy in humans in the absence of increased muscle protein breakdown. J Cachexia Sarcopenia Muscle *13*, 2005-2016.

Buccitelli, C., and Selbach, M. (2020). mRNAs, proteins and the emerging principles of gene expression control. Nat.Rev.Genet. *21*, 630-644.

Casuso, R.A., Huertas, J.R., and Aragon-Vela, J. (2024). The role of muscle disuse in muscular and cardiovascular fitness: A systematic review and meta-regression. Eur J Sport Sci *24*, 812-823.

Chiara, F., Castellaro, D., Marin, O., Petronilli, V., Brusilow, W.S., Juhaszova, M., Sollott, S.J., Forte, M., Bernardi, P., and Rasola, A. (2008). Hexokinase II detachment from mitochondria triggers apoptosis through the permeability transition pore independent of voltage-dependent anion channels. PLoS One *3*, e1852.

Chopard, A., Arrighi, N., Carnino, A., and Marini, J.F. (2005). Changes in dysferlin, proteins from dystrophin glycoprotein complex, costameres, and cytoskeleton in human soleus and vastus lateralis muscles after a long-term bedrest with or without exercise. FASEB J *19*, 1722-1724.

Chopard, A., Lecunff, M., Danger, R., Lamirault, G., Bihouee, A., Teusan, R., Jasmin, B.J., Marini, J.F., and Leger, J.J. (2009). Large-scale mRNA analysis of female skeletal muscles during 60 days of bed rest with and without exercise or dietary protein supplementation as countermeasures. Physiol Genomics *38*, 291-302.

Crossland, H., Skirrow, S., Puthucheary, Z.A., Constantin-Teodosiu, D., and Greenhaff, P.L. (2019). The impact of immobilisation and inflammation on the regulation of muscle mass and insulin resistance: different routes to similar end-points. J Physiol *597*, 1259-1270.

Deane, C.S., Piasecki, M., and Atherton, P.J. (2024). Skeletal muscle immobilisation-induced atrophy: mechanistic insights from human studies. Clin Sci (Lond) *138*, 741-756.

Delfinis, L.J., Khajehzadehshoushtar, S., and Perry, C.G.R. (2025). Perspectives on the interpretation of mitochondrial responses during skeletal muscle disuse-induced atrophy. J Physiol *603*, 3679-3699.

Doering, T.M., Thompson, J.M., Budiono, B.P., MacKenzie-Shalders, K.L., Zaw, T., Ashton, K.J., and Coffey, V.G. (2022). The muscle proteome reflects changes in mitochondrial function, cellular stress and proteolysis after 14 days of unilateral lower limb immobilization in active young men. PLoS One *17*, e0273925.

Fitts, R.H., Trappe, S.W., Costill, D.L., Gallagher, P.M., Creer, A.C., Colloton, P.A., Peters, J.R., Romatowski, J.G., Bain, J.L., and Riley, D.A. (2010). Prolonged space flight-induced alterations in the structure and function of human skeletal muscle fibres. J Physiol *588*, 3567-3592.

Fornasiero, E.F., Mandad, S., Wildhagen, H., Alevra, M., Rammner, B., Keihani, S., Opazo, F., Urban, I., Ischebeck, T., Sakib, M.S., et al. (2018). Precisely measured protein lifetimes in the mouse brain reveal differences across tissues and subcellular fractions. Nat Commun *9*, 4230.

Franchi, M.V., Candia, J., Sarto, F., Sirago, G., Valli, G., Paganini, M., Hartnell, L., Giacomello, E., Toniolo, L., Monti, E., et al. (2025). Previous short-term disuse dictates muscle gene expression and physiological adaptations to subsequent resistance exercise. J Physiol *603*, 3725-3753.

Gram, M., Vigelso, A., Yokota, T., Hansen, C.N., Helge, J.W., Hey-Mogensen, M., and Dela, F. (2014). Two weeks of one-leg immobilization decreases skeletal muscle respiratory capacity equally in young and elderly men. Exp Gerontol *58*, 269-278.

Hardy, E.J.O., Inns, T.B., Hatt, J., Doleman, B., Bass, J.J., Atherton, P.J., Lund, J.N., and Phillips, B.E. (2022). The time course of disuse muscle atrophy of the lower limb in health and disease. J Cachexia Sarcopenia Muscle *13*, 2616-2629.

Hendrickse, P.W., Wust, R.C.I., Ganse, B., Giakoumaki, I., Rittweger, J., Bosutti, A., and Degens, H. (2022). Capillary rarefaction during bed rest is proportionally less than fibre atrophy and loss of oxidative capacity. J Cachexia Sarcopenia Muscle *13*, 2712-2723.

Hikida, R.S., Gollnick, P.D., Dudley, G.A., Convertino, V.A., and Buchanan, P. (1989). Structural and metabolic characteristics of human skeletal muscle following 30 days of simulated microgravity. Aviat Space Environ Med *60*, 664-670.

Kozlovskaya, I., Sayenko, I.V., Sayenko, D., Miller, T.F., Khusnutdinova, D.R., and Melnik, K.A. (2007). Role of support afferentation in control of the tonic muscle activity. Acta Astronautica *60*, 285-294.

Kurochkina, N.S., Orlova, M.A., Vigovskiy, M.A., Zgoda, V.G., Vepkhvadze, T.F., Vavilov, N.E., Makhnovskii, P.A., Grigorieva, O.A., Boroday, Y.R., Philippov, V.V., et al. (2024). Age-related changes in human skeletal muscle transcriptome and proteome are more affected by chronic inflammation and physical inactivity than primary aging. Aging Cell *23*, e14098.

Lambertz, D., Perot, C., Kaspranski, R., and Goubel, F. (2001). Effects of long-term spaceflight on mechanical properties of muscles in humans. J Appl Physiol (1985) *90*, 179-188.

Lawler, J.M., Song, W., and Kwak, H.B. (2006). Differential response of heat shock proteins to hindlimb unloading and reloading in the soleus. Muscle Nerve *33*, 200-207.

LeBlanc, A.D., Schneider, V.S., Evans, H.J., Pientok, C., Rowe, R., and Spector, E. (1992). Regional changes in muscle mass following 17 weeks of bed rest. J Appl Physiol (1985) *73*, 2172-2178.

Leppek, K., Das, R., and Barna, M. (2018). Functional 5' UTR mRNA structures in eukaryotic translation regulation and how to find them. Nat.Rev.Mol.Cell Biol. *19*, 158-174.

Liu, Y., Beyer, A., and Aebersold, R. (2016). On the Dependency of Cellular Protein Levels on mRNA Abundance. Cell *165*, 535-550.

Makhnovskii, P.A., Zgoda, V.G., Bokov, R.O., Shagimardanova, E.I., Gazizova, G.R., Gusev, O.A., Lysenko, E.A., Kolpakov, F.A., Vinogradova, O.L., and Popov, D.V. (2020). Regulation of Proteins in Human Skeletal Muscle: The Role of Transcription. Sci Rep *10*, 3514.

Mann, C.J., Perdiguero, E., Kharraz, Y., Aguilar, S., Pessina, P., Serrano, A.L., and Munoz-Canoves, P. (2011). Aberrant repair and fibrosis development in skeletal muscle. Skelet Muscle *1*, 21.

Marusic, U., Narici, M., Simunic, B., Pisot, R., and Ritzmann, R. (2021). Nonuniform loss of muscle strength and atrophy during bed rest: a systematic review. J Appl Physiol (1985) *131*, 194-206.

McKee, T.J., Perlman, G., Morris, M., and Komarova, S.V. (2019). Extracellular matrix composition of connective tissues: a systematic review and meta-analysis. Sci Rep *9*, 10542.

Michelucci, A., Liang, C., Protasi, F., and Dirksen, R.T. (2021). Altered Ca(2+) Handling and Oxidative Stress Underlie Mitochondrial Damage and Skeletal Muscle Dysfunction in Aging and Disease. Metabolites *11*.

Mikines, K.J., Richter, E.A., Dela, F., and Galbo, H. (1991). Seven days of bed rest decrease insulin action on glucose uptake in leg and whole body. J Appl Physiol (1985) *70*, 1245-1254.

Miotto, P.M., McGlory, C., Bahniwal, R., Kamal, M., Phillips, S.M., and Holloway, G.P. (2019). Supplementation with dietary omega-3 mitigates immobilization-induced reductions in skeletal muscle mitochondrial respiration in young women. FASEB J *33*, 8232-8240.

Morgenstern, M., Peikert, C.D., Lubbert, P., Suppanz, I., Klemm, C., Alka, O., Steiert, C., Naumenko, N., Schendzielorz, A., Melchionda, L., et al. (2021). Quantitative high-confidence human mitochondrial proteome and its dynamics in cellular context. Cell Metab *33*, 2464-2483 e2418.

Noone, J., Damiot, A., Kenny, H., Chery, I., Zahariev, A., Normand, S., Crampes, F., de Glisezinski, I., Rochfort, K.D., Laurens, C., et al. (2025). The impact of 60 days of -6 degrees head down tilt bed rest on mitochondrial content, respiration and regulators of mitochondrial dynamics. J Physiol *603*, 3777-3794.

Ogneva, I.V., Kurushin, V.A., Altaeva, E.G., Ponomareva, E.V., and Shenkman, B.S. (2009). Effect of short-term gravitational unloading on rat and mongolian gerbil muscles. J Muscle Res Cell Motil *30*, 261-265.

Pavan, P., Monti, E., Bondi, M., Fan, C., Stecco, C., Narici, M., Reggiani, C., and Marcucci, L. (2020). Alterations of Extracellular Matrix Mechanical Properties Contribute to Age-Related Functional Impairment of Human Skeletal Muscles. Int J Mol Sci *21*.

Pomella, S., Cassandri, M., Antoniani, F., Crotti, S., Mediani, L., Silvestri, B., Medici, M., Rota, R., Rosa, A., and Carra, S. (2023). Heat Shock Proteins: Important Helpers for the Development, Maintenance and Regeneration of Skeletal Muscles. Muscles *2*, 187-203.

Popov, D.V., Makhnovskii, P.A., Zgoda, V.G., Gazizova, G.R., Vepkhvadze, T.F., Lednev, E.M., Motanova, E.S., Lysenko, E.A., Orlov, O.I., and Tomilovskaya, E.S. (2023). Rapid changes in transcriptomic profile and mitochondrial function in human soleus muscle after 3-day dry immersion. J Appl Physiol (1985) *134*, 1256-1264.

Puchkova, A.A., Shpakov, A.V., Baranov, V.M., Katuntsev, V.P., Stavrovskaya, D.M., Primachenko, G.K., Gorbachev, V.P., Tomilovskaya, E.S., and Orlov, O.I. (2024). General results of a 21-day head-down bed rest study without use of countermeasures. Human Physiology *50*, 808-816.

Ried-Larsen, M., Aarts, H.M., and Joyner, M.J. (2017). Effects of strict prolonged bed rest on cardiorespiratory fitness: systematic review and meta-analysis. J Appl Physiol (1985) *123*, 790-799.

Rolfs, Z., Frey, B.L., Shi, X., Kawai, Y., Smith, L.M., and Welham, N.V. (2021). An atlas of protein turnover rates in mouse tissues. Nat Commun *12*, 6778.

Schwanhausser, B., Busse, D., Li, N., Dittmar, G., Schuchhardt, J., Wolf, J., Chen, W., and Selbach, M. (2011). Global quantification of mammalian gene expression control. Nature *473*, 337-342.

Senf, S.M. (2013). Skeletal muscle heat shock protein 70: diverse functions and therapeutic potential for wasting disorders. Front Physiol *4*, 330.

Singh, K., and Hood, D.A. (2011). Effect of denervation-induced muscle disuse on mitochondrial protein import. Am J Physiol Cell Physiol *300*, C138-145.

Thot, G.K., Berwanger, C., Mulder, E., Lee, J.K., Lichterfeld, Y., Ganse, B., Giakoumaki, I., Degens, H., Duran, I., Schonau, E., et al. (2021). Effects of long-term immobilisation on endomysium of the soleus muscle in humans. Exp Physiol *106*, 2038-2045.

Tomilovskaya, E., Shigueva, T., Sayenko, D., Rukavishnikov, I., and Kozlovskaya, I. (2019). Dry Immersion as a Ground-Based Model of Microgravity Physiological Effects. Front Physiol *10*, 284.

Trappe, T.A., Minchev, K., Perkins, R.K., Lavin, K.M., Jemiolo, B., Ratchford, S.M., Claiborne, A., Lee, G.A., Finch, W.H., Ryder, J.W., et al. (2024). NASA SPRINT exercise program efficacy for vastus lateralis and soleus skeletal muscle health during 70 days of simulated microgravity. J Appl Physiol (1985) *136*, 1015-1039.

Vyssokikh, M.Y., Holtze, S., Averina, O.A., Lyamzaev, K.G., Panteleeva, A.A., Marey, M.V., Zinovkin, R.A., Severin, F.F., Skulachev, M.V., Fasel, N., et al. (2020). Mild depolarization of the inner mitochondrial membrane is a crucial component of an anti-aging program. Proc Natl Acad Sci U S A *117*, 6491-6501.

Xu, Z., Fu, T., Guo, Q., Zhou, D., Sun, W., Zhou, Z., Chen, X., Zhang, J., Liu, L., Xiao, L., et al. (2022). Disuse-associated loss of the protease LONP1 in muscle impairs mitochondrial function and causes reduced skeletal muscle mass and strength. Nat Commun *13*, 894.

Yu, S.H., Kyriakidou, P., and Cox, J. (2020). Isobaric Matching between Runs and Novel PSM-Level Normalization in MaxQuant Strongly Improve Reporter Ion-Based Quantification. J Proteome Res *19*, 3945-3954.

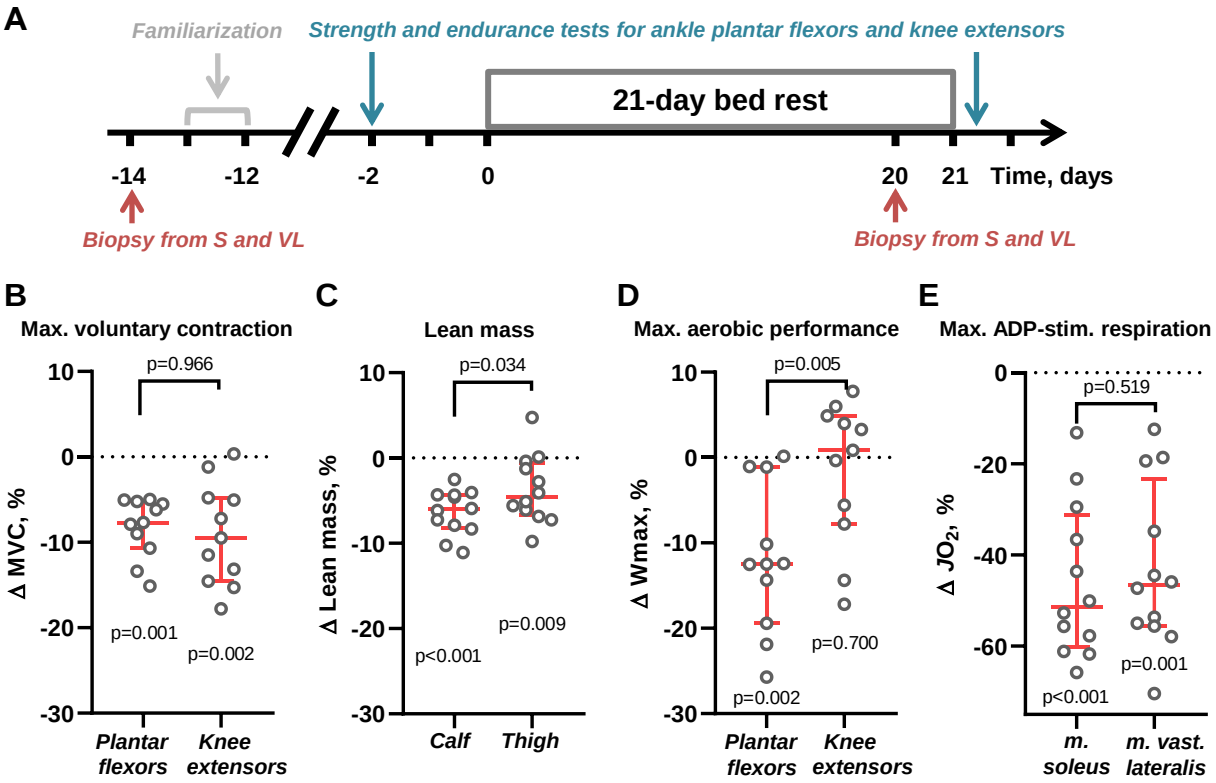
A
Familiarization
Strength and endurance tests for ankle plantar flexors and knee extensors
21-day bed rest
-14
-12
-2
0
20
21
Time, days
Biopsy from S and VL
Biopsy from S and VL
B
Max. voluntary contraction
Δ MVC, %
p=0.966
p=0.001
p=0.002
Plantar flexors
Knee extensors
C
Lean mass
Δ Lean mass, %
p=0.034
p<0.001
p=0.009
Calf
Thigh
D
Max. aerobic performance
Δ Wmax, %
p=0.005
p=0.002
p=0.700
Plantar flexors
Knee extensors
E
Max. ADP-stim. respiration
Δ JO2, %
p=0.519
p<0.001
p=0.001
m. soleus
m. vast. lateralis

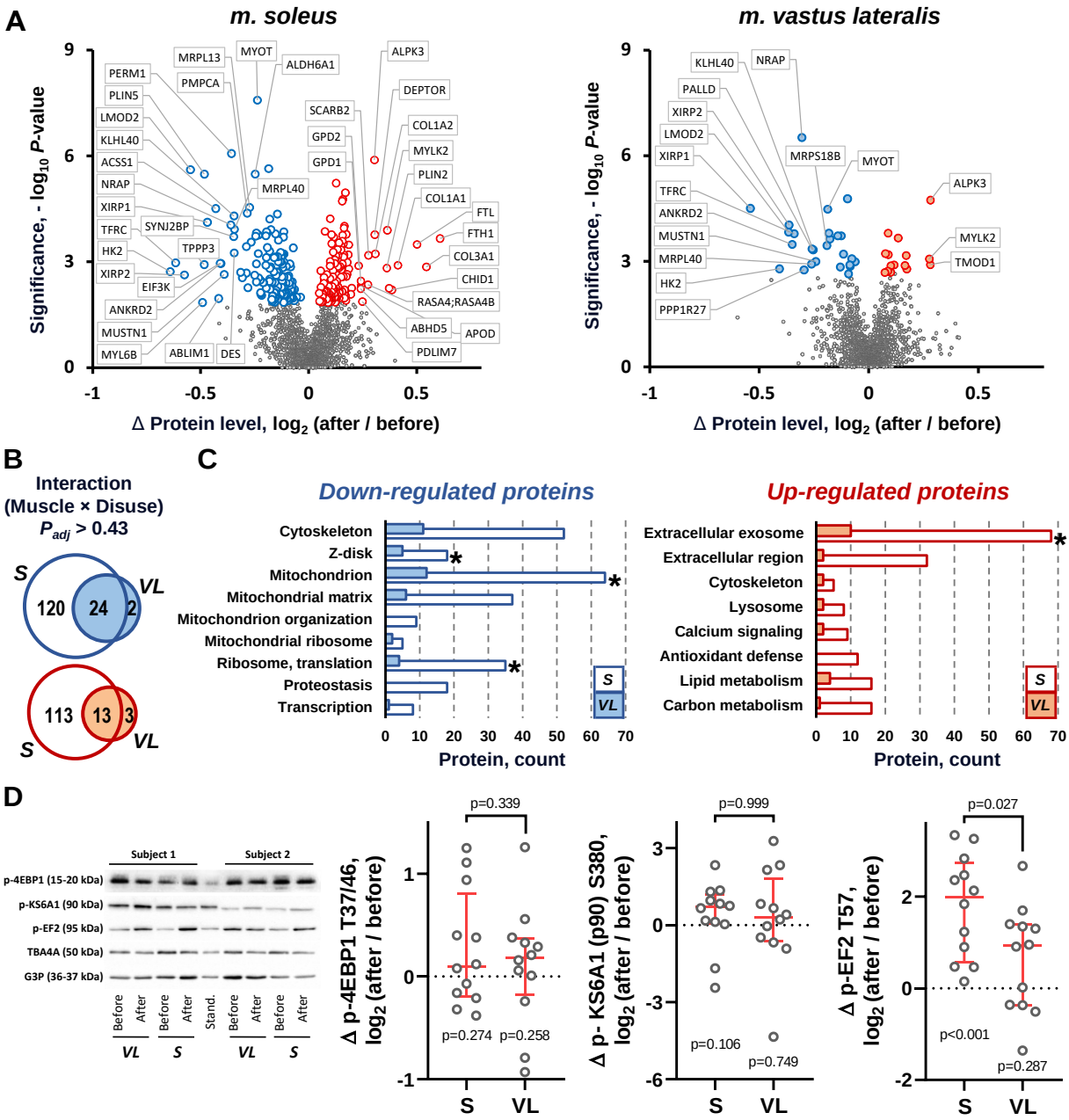
A
m. soleus
m. vastus lateralis
Significance, - log10 P-value
Δ Protein level, log2 (after / before)
MRPL13
MYOT
ALDH6A1
ALPK3
PERM1
PMPCA
DEPTOR
PLIN5
SCARB2
LMOD2
COL1A2
GPD2
KLHL40
MYLK2
ACSS1
GPD1
PLIN2
NRAP
MRPL40
COL1A1
XIRP1
FTL
TFRC
SYNJ2BP
FTH1
HK2
TPPP3
COL3A1
XIRP2
CHID1
EIF3K
RASA4;RASA4B
ANKRD2
ABHD5
APOD
MUSTN1
MYL6B
ABLIM1
DES
PDLIM7
KLHL40
NRAP
PALLD
XIRP2
LMOD2
XIRP1
MRPS18B
MYOT
ALPK3
TFRC
ANKRD2
MYLK2
MUSTN1
TMOD1
MRPL40
HK2
PPP1R27
B
Interaction
(Muscle × Disuse)
Padj > 0.43
S
VL
120
24
2
113
13
3
C
Down-regulated proteins
Up-regulated proteins
Cytoskeleton
Z-disk
Mitochondrion
Mitochondrial matrix
Mitochondrion organization
Mitochondrial ribosome
Ribosome, translation
Proteostasis
Transcription
Extracellular exosome
Extracellular region
Cytoskeleton
Lysosome
Calcium signaling
Antioxidant defense
Lipid metabolism
Carbon metabolism
Protein, count
D
Subject 1
Subject 2
p-4EBP1 (15-20 kDa)
p-KS6A1 (90 kDa)
p-EF2 (95 kDa)
TBA4A (50 kDa)
G3P (36-37 kDa)
Before
After
Stand.
Δ p-4EBP1 T37/46, log2 (after / before)
Δ p- KS6A1 (p90) S380, log2 (after / before)
Δ p-EF2 T57, log2 (after / before)
p=0.339
p=0.274
p=0.258
p=0.999
p=0.106
p=0.749
p=0.027
p<0.001
p=0.287

A

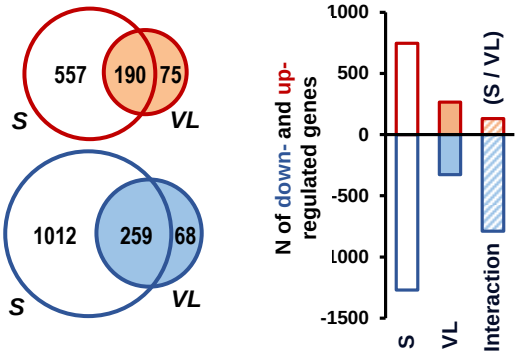

B

Interaction: over-activated in S vs. VL

Term		Count
GO:0005886	Plasma membrane	50
GO:0005615	Extracellular space	22
KW-0206	Cytoskeleton	22
GO:0006954	Inflammatory response	12
GO:0006955	Immune response	10

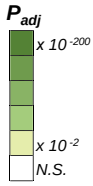

C

Interaction: over-suppressed in S vs. VL

Term		Count
GO:0005739	Mitochondrion	444
GO:0005743	mitochondrial inner membrane	222
GO:0005759	Mitochondrial matrix	168
hsa00190	Oxidative phosphorylation	76
GO:0032543	Mitochondrial translation	58
GO:0005758	Mitochondrial intermembrane space	36
GO:0005741	Mitochondrial outer membrane	32
GO:0007005	Mitochondrion organization	28
GO:0006099	Tricarboxylic acid cycle	18
GO:0006626	Protein targeting to mitochondrion	16
GO:0006412	Translation	41
hsa03010	Ribosome	31
KW-0443	Lipid metabolism	62
hsa01230	Biosynthesis of amino acids	13
hsa00280	Valine, leucine and isoleucine degradation	27
KW-0576	Peroxisome	20

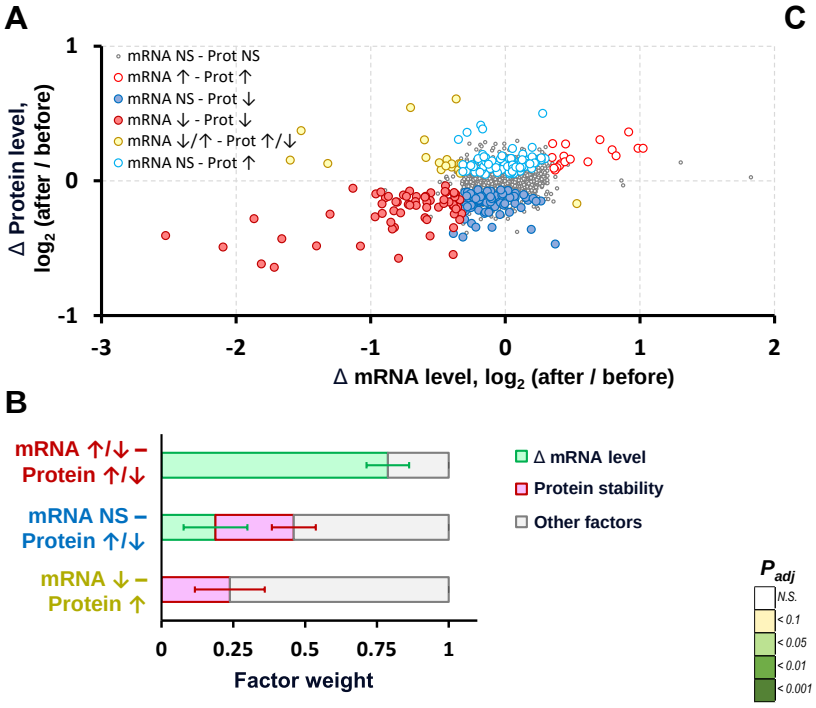

C

Term		mRNA Down	mRNA NS	mRNA Up	mRNA NS	mRNA Down
		Prot. Down		Prot. Up		
KW-0496	Mitochondrion	36				
GO:0005739	mitochondrion	41				
GO:0005759	mitochondrial matrix	17				
KW-0963	Cytoplasm		54			
GO:0005737	cytoplasm		51			
hsa03010	Ribosome		15			
GO:0005840	ribosome		16			
GO:1990904	ribonucleoprotein complex		14			
GO:0006412	translation		18			
GO:0002181	cytoplasmic translation		15			
GO:0022626	cytosolic ribosome		13			
GO:0022627	cytosolic small ribosomal subunit		8			
GO:0015935	small ribosomal subunit		6			
GO:0022625	cytosolic large ribosomal subunit		7			
GO:0030018	Z disc		12			
GO:0005925	focal adhesion		17			
KW-0517	Myogenesis		4			
KW-0221	Differentiation		7			
GO:0070062	extracellular exosome				49	
KW-0443	Lipid metabolism					5